PROCEEDINGS OF SCIENCE

Study of High Lying Resonances in ^{9}Be by the Measurement of (p,p), (p,α) and (p,d) Reactions

A. Lépine-Szily [a]*, E. Leistenschneider [b], P. Descouvemont [c], D. R. Mendes Jr [d], R. Lichtenthäler [a], M. A. G. Alvarez [a], R. Pampa Condori [ad], P. N. de Faria [d], K. C. C. Pires [a], V. Scarduelli [a], V. A. B. Zagatto [ad], N. Desmukh [a], V. Morcelle [e], M. C. Morais [f], J. M. B. Shorto [g], V. Guimarães [a], M. Assunção [h]

[a] *Instituto de Física da Universidade de São Paulo, 05315-970, São Paulo, SP, Brazil*
[b] *The University of British Columbia, Department of Physics and Astronomy, Vancouver, BC V6T 1Z1, Canada*
[c] *Physique Nucléaire Théorique et Physique Mathématique, C.P. 229, Université Libre de Bruxelles (ULB), B 1050 Brussels, Belgium*
[d] *Instituto de Física, Universidade Federal Fluminense, Niterói RJ 24210-340, Brazil*
[e] *Universidade Federal Rural de Rio de Janeiro- RJ, Brazil*
[f] *Universidade Federal Fluminense, Instituto do Noroeste Fluminense de Ensino Superior, CEP 28470-000, Santo Antonio de Padua, RJ, Brasil.*
[g] *Instituto de Pesquisas Energèticas e Nucleares, CNEN, São Paulo, SP, Brazil*
[h] *Departamento de Ciências Exatas e da Terra, Universidade Federal de São Paulo, Campus Diadema, São Paulo, Brazil*
E-mail: `alinka@if.usp.br`

The (p, p), (p, α) and (p, d) reactions on ^{8}Li were measured at low energies. The experiment was performed using a thick $[CH_2]_n$ target and a radioactive ^{8}Li beam available at the RIBRAS facility of São Paulo . This experiment represents an upgrade of a previous experiment, where only the ^{8}Li(p,α)^{5}He cross section was measured. High lying resonances of ^{9}Be, which are still uncertain, could be studied in this way. The detection of several reaction channels allows a reliable determination of the resonance parameters, such as energy, width and spin-parity. In the deuteron channel we could observe the same resonance decaying to d+^{7}Li$_{gs}$ and to d+^{7}Li*. The properties of the resonances are determined by a R-matrix analysis, which provides evidence for a significant clustering as well in the (p, α) as in the (p, d) channels. The experimental data and the multi-channel R-matrix analysis will be presented.

The 26th International Nuclear Physics Conference
11-16 September, 2016
Adelaide, Australia

*Speaker.

PoS(INPC2016)223

1. Introduction

The study of exotic nuclei is one of the forefronts of current research in nuclear physics [1]. Recently developed facilities, worldwide, which produce beams of radioactive nuclei, provide unique opportunities to probe new aspects of nuclear physics [2, 3, 4] and of nuclear astrophysics [5]. The discovery of halo nuclei [6] thirty years ago triggered many experimental and theoretical works to search for nuclei with unusual properties, such as an anomalously large radius, or an enhanced breakup cross section. Nowadays, several nuclei, such as ^{6}He, ^{11}Li or ^{14}Be, are well known to present a halo structure, where a core is surrounded by one or two nucleons. Another unexpected development of nuclear structure, due to the availability of radioactive beams, is the evolution of the shell structures [7]. In comparison with stable nuclei, isotopes close to the drip lines do not follow the same shell evolution, and the magic numbers are different.

Exotism in light or medium mass nuclei (A<60) is, in general, associated with an N/Z ratio fairly different from unity. For stable isotopes, such as ^{12}C ($N/Z = 1$) or ^{15}N ($N/Z = 1.14$), this ratio is close, or equal, to 1. However, for nuclei located near (or at) the driplines, N/Z can be very different from 1 (for example, $N/Z = 3$ for ^{8}He and ^{24}O, $N/Z = 0.5$ for ^{9}C). These properties provide strong constraints on structure models, and, in particular, on the nucleon-nucleon interaction near the driplines.

One of the concepts of exotism is related to unusual structures observed at the limits of the stability lines. Examples are the neutron halo structures already mentioned above (^{6}He, ^{11}Li or ^{14}Be among other) or another typical example is ^{8}B which is seen as a ^{7}Be core surrounded by a proton located at large distances. This two-body structure, involving an inert core and a nucleon, is relatively frequent in the low-mass region. However, this concept of exotism can be extended by considering either core excitations, or a larger number of constituents. Recently, core excitation has been observed by inelastic scattering in ^{18}Ne+p [8]. Modern scattering calculations also involve core excitations, as an important contribution to the process [9, 10]. On the other hand, most exotic nuclei present a two- or three-body structure. Some nuclei, such as ^{10}C, can even be considered as Borromean four-body systems (none of the two- or three-body substructures of the $\alpha+\alpha+p+p$ system is bound), but there is currently no experimental evidence for a four-body clustering.

In the present work, our goal is to investigate exotic states in ^{9}Be near the proton threshold, possibly characterized by a multi-cluster structure. To this aim, we use three reactions involving a radioactive ^{8}Li beam on a proton target. By observing simultaneously the protons, the alpha particles, and the deuterons, we determine the ^{8}Li$(p,p)^8$Li elastic scattering, and the ^{8}Li$(p,\alpha)^5$He and ^{8}Li$(p,d)^7$Li transfer cross sections. At low proton energies, these reactions probe the ^{9}Be spectrum around $E_x \approx 18-20$ MeV. This energy region was previously studied by our group [11], but was limited to the ^{8}Li$(p,\alpha)^5$He cross section.

The *R*-matrix theory [12, 13] is an ideal tool to analyze low-energy data. It is based on the existence of two regions, separated by the channel radius a. In the internal region, the physics of the problem is described by real and energy-independent parameters. In the external region, the colliding nuclei interact through the Coulomb force only. These *R*-matrix parameters, energies and reduced widths, are associated with properties of ^{9}Be states. The simultaneous analysis of (p,p), (p,d) and (p,α) data with common parameters provides constraints on these parameters. For example, the energies and proton widths of the resonances are common to the three processes.

PoS(INPC2016)223

In its ground state, ^{9}Be can be accurately described by an $\alpha+\alpha+n$ three-body model [15]. This structure corresponds to a Borromean system, for which none of the two-body subsystems ($\alpha+\alpha$ and $\alpha+n$) is bound. At high excitation energies (the proton threshold energy is $Q_p = 16.89$ MeV), the ^{9}Be spectrum is, however, more complex, and other cluster structures can be expected. The availability of (p,p), (p,d) and (p,α) cross sections obtained simultaneously in the same energy range provides an excellent opportunity to probe the ^{9}Be structure in this energy region.

2. Experimental method

The experiment was performed at the "Radioactive Ion Beams in Brazil" (RIBRAS) facility, installed at the 8-UD Pelletron Tandem Laboratory of the University of São Paulo [4]. A short description of the experimental setup is given here, and more detail can be found in Refs. [16, 17, 4]. The most important components of this facility are two superconducting solenoids with a 6.5T maximum central field, and a 30 cm clear warm bore.

The measurement of the ^{8}Li$(p,p)^8$Li, ^{8}Li$(p,d)^7$Li and ^{8}Li$(p,\alpha)^5$He excitation functions was performed using the so-called "TTIK method" (Thick-Target Inverse Kinematics), with a ^{8}Li secondary beam impinging on a 6.8 mg/cm^2 thick $[CH_2]_n$ polyethylene foil. In the TTIK method, the whole excitation function can be obtained from the energy spectrum of the light ejectiles. The light ejectiles, protons, deuterons, and α-particles were detected at forward laboratory angles ($\theta_{\rm lab} = 10^\circ$ and 18°).

The ^{8}Li^{3+} secondary beam was produced by the ^{9}Be(^{7}Li,^{8}Li)^{8}Be transfer reaction ($Q = 0.367$ MeV). The primary beam (^{7}Li) was stopped and integrated in a Faraday cup, which stops all particles in the angular region from 0° to 2°. The angular acceptance of the system in the present experiment, was $2^\circ - 6^\circ$ in the entrance and $1.5^\circ - 3.5^\circ$ at the end of the solenoid. The secondary beams are selected and focused by the solenoids from their magnetic rigidity.

The ^{8}Li production rate was maximized by varying the solenoid current, and measured through the Rutherford elastic scattering on a ^{197}Au secondary target. Measurements with the gold target of 5.3 mg/cm^2 thickness were performed several times, and the production rate was quite constant during each run (between 10^5 and 5×10^5 pps, depending on the energy). The measurements of the ^{8}Li$+p$ cross sections were performed with a clean ($\approx$ 99%) radioactive ^{8}Li beam, which was produced using both solenoids, and an Al degrader, with thickness of 7.5 mg/cm^2, between them. Measurements with a thick natural carbon target were also performed in order to subtract possible reactions with the carbon present in the polyethylene target. The particles produced by the secondary beam on the reaction targets, located in the center of the scattering chamber after the second solenoid, were detected in two $\Delta E-E$ Si telescopes located respectively at $\theta_{\rm lab} = 10^\circ$ and 18°. The ΔE and E detectors have thicknesses of 50 μm and 1000 μm, respectively, with geometrical solid angles of 12.5 and 12.0 msr. The detectors were calibrated using standard α-particle source.

3. Data analysis and results

On Fig. 1 (a) and (b) we show the bi-dimensional identification spectrum of the Si telescope at $\theta_{\rm lab} = 10^\circ$. It was obtained, using the thick $[CH_2]_n$ target and the secondary beam with $E_{\rm lab}$ = 18.7

MeV. Despite the important purification of the secondary beam, the presence of light contaminant particles, such as protons, deuterons, tritons and α-particles, cannot be completely avoided at very forward angles as 10° , due to the in-flight method and the large acceptance of the solenoids. These particles could be produced in the production target, or in the degrader, and be transmitted along the axis of the solenoids. On Fig. 1 (c) the bi-dimensional identification spectrum of the Si telescope at $\theta_{\text{lab}} = 18^\circ$ is shown, using the thick $[CH_2]_n$ target and the secondary beam with E_{lab} = 16.0 MeV. This spectrum is free of light contaminant particles, when compared to Fig 1 (a,b). All three spectra show a very good identification resolution, and the protons resulting from the $^8\text{Li}(p,p)^8\text{Li}$ scattering are well separated from other light particles. Due to contamination the proton strip on Fig.1 (b) shows a very large number of counts, when compared to deuterons or alphas, very differently from the spectrum obtained at 18°, seen on Fig. 1 (c). Also one can see strong peaks in the strips of deuterons, tritons and α-particles, which correspond to particles with the correct energy to be transmitted through the second solenoid. These strong peaks are absent on Fig. 1 (c). The light particles (protons, deuterons), which were transmitted through the solenoids or passed along the axis of the solenoids could be eliminated positioning the Si telescope at 18°.

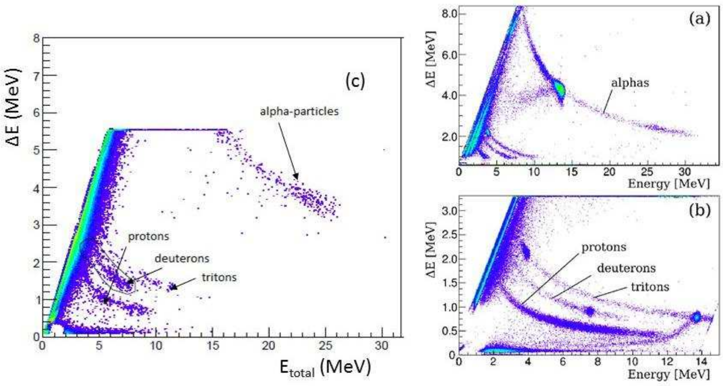

Figure 1: (Color online). (a) Bi-dimensional identification spectrum obtained using a Si telescope at $\theta_{\text{lab}} = 10^\circ$ in the scattering chamber after the second solenoid, with the secondary beam of E_{lab} = 18.7 MeV focused on a $[CH_2]_n$ target. Fig. 1(b) presents a spectrum with higher gain in the ΔE channel (y axis), where α particles are cut off. The strongest peaks in the alpha, triton and deuteron lines are due to contaminant beams. Fig. 1(c) presents the identification spectrum measured at $\theta_{\text{lab}} = 18^\circ$ with the secondary beam of E_{lab} = 16.0 MeV. In all three spectra the energies on the x-axis are the total detected energies in the Si telescope.

Two incident energies were used in this experiment, $E_{\text{lab}}(^8\text{Li}) = 18.7$ and 16.0 MeV, and the resulting excitation functions are obtained from the superposition of both data sets. The measurements with the Si telescope at 18° were performed only at the lower energy, at 16.0 MeV.

In the ^{8}Li(p,α)^{5}He reaction, the recoiling ^{5}He is unbound and disintegrates into an α-particle and a neutron. Similarly, in the ^{1}H(^{8}Li,^{8}Be)n reaction, the ^{8}Be is unbound breaking into two α-particles. The contribution of these α-particles, as well as the continuous energy distributions of α-particles resulting from the 3-body break-up, were calculated and subtracted from the energy spectra. All details of these calculations can be obtained in the reference of Mendes et al. [11]. We discovered that the published cross section is affected by an unnecessary normalization factor $dE(^8\text{Li})/dE_\alpha$, associated with the conversion from the alpha energy to the ^{8}Li energy. This factor

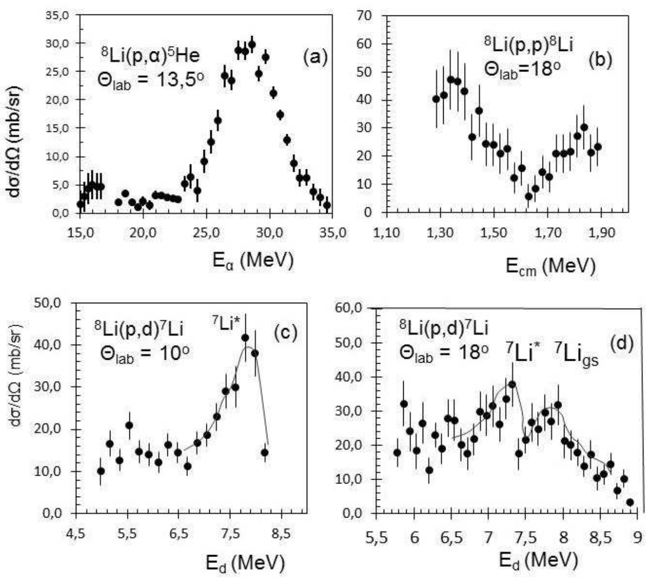

Figure 2: (a) ^{8}Li$(p,\alpha)^5$He, Ref [11]), (b) ^{8}Li$(p,p)^8$Li, and (c,d) ^{8}Li$(p,d)^7$Li experimental cross sections at angles indicated on the figure. The ^{8}Li$(p,d)^7$Li excitation functions are plotted as a function of the deuteron energy in the reaction. The one measured at $\theta_{\rm lab} = 10^\circ$ is cut at E$_{\rm d}$=8.3 MeV, due to the presence of an adjacent strong contaminant peak (see Figure 1 (b).

is larger than unity above 1 MeV, and its removal reduces the cross section. The corrected values are presented in Fig. 2(a). These data have better statistics than our new measurements and we are confident in their absolute value, since they were measured in a chamber after the first solenoid, where the production rate was well tested by elastic angular distributions on a gold target. The absolute values of the more recent measurements performed with a purified ^{8}Li beam at $\theta_{\rm lab} = 10^\circ$ and 18° are not well determined. Due to the low energy of ^{8}Li and thick Al degrader and gold target, the angular straggling of the scattered ^{8}Li beam was very large. The effective scattering angle, which is calculated using a Monte-Carlo code, which takes into account all details of the set-up, could not be determined precisely due to the large angular uncertainty of the beam. Thus the value of the incident ^{8}Li beam intensity is quite uncertain and so the absolute value of the cross section also. However the relative values are not affected by this constant factor. The normalization of our ^{8}Li$(p,\alpha)^5$He results on the cross section of the ^{8}Li$(p,\alpha)^5$He of Ref. [11] determined our absolute values. The uncertainty of this normalization process is less than 30%.

The ^{8}Li$(p,p)^8$Li reaction was measured at $E_{\rm lab}(^8{\rm Li}) = 16.0$ MeV and $\theta_{\rm lab} = 18^\circ$, while the ^{8}Li$(p,d)^7$Li reaction was measured at the two incident energies and the two detection angles. The cross sections are displayed in Fig. 2.

We present the ^{8}Li$(p,\alpha)^5$He data in α-particle energy and the ^{8}Li$(p,d)^7$Li data in deuteron energy because in our analysis, we take into account the recoiling nuclei, respectively ^{5}He and ^{7}Li, in their ground state and in their first excited state. The ejectiles have different energies following the recoil excitation. In Fig. 2(b) we see a strong minimum in the ^{8}Li$(p,p)^8$Li cross section around E$_{\rm cm}$= 1.63 MeV. In Fig. 2(c) and (d) we present excitation functions of the reaction ^{8}Li$(p,d)^7$Li, measured at $\theta_{\rm lab}$= 10° and 18° respectively. On the energy spectrum (c) a strong contamination peak appears at $E_d > 8.3$ MeV, however there is a clear peak next to it, at E_d=7.9 MeV, which corresponds, following kinematic calculations, to the deuteron channel with the ^{7}Li* nucleus in its first excited state (E*=0.478 MeV). On the energy spectrum (d), measured at $\theta_{\rm lab}$= 18° two peaks can be observed, which correspond to the d+^{7}Li* and the d+^{7}Li$_{gs}$ channels.

4. Multi-channel R-matrix analysis

The present cross sections were analyzed in terms of a multichannel R-matrix calculation. The phenomenological R-matrix method represents a powerful tool to derive resonance properties from low-energy cross sections [13, 18]. The availability of cross sections of three different reactions at several angles in the same energy range provides an additional and strong constrain on this analysis. For a given partial wave $J\pi$, the R-matrix involving the initial channel i and the final channel f is given by

$$R_{if}(E) = \sum_{\lambda=1}^{N} \frac{\gamma_i^\lambda \gamma_f^\lambda}{E_\lambda - E}, \tag{4.1}$$

where index λ refers to the N poles, associated with resonances and bound states. The energies are denoted as E_λ, and the reduced partial widths in channel c as γ_c^λ. The R-matrix parameters $(E_\lambda, \gamma_c^\lambda)$ are real and energy independent. They are specific to the R-matrix theory, and depend on the channel radius. They can be transformed into “observed" parameters, the resonance energies E_r and the partial widths Γ_c, by well known techniques [19]. The scattering cross sections are then determined from the scattering matrices in the different partial waves [12, 13]. The R-matrix code [13] was modified in order to include the channels, where the recoiling nuclei are in excited states. The center of mass energy above the reaction threshold was transformed into laboratory energy of the ejectiles, which are different when the recoil is excited, even if the resonance energy is the same. The present analysis involves five channels: proton $(c = 1)$, α $(c = 2)$, α' $(c = 3)$, d $(c = 4)$ and d' $(c = 5)$, where α' and d' refer, respectively, to the recoiling nuclei ^{5}He and ^{7}Li in their first excited states. The cross sections calculated by the R-matrix analysis are displayed in Fig. 3, and the resonance properties deduced from the R-matrix analysis are presented on Table 1.

For the ^{8}Li$(p,d)^7$Li cross sections, we have summed the R-matrix contributions of the ^{7}Li ground and first excited states. The $5/2^-$ resonance near $E_{\rm c.m.} = 0.42$ MeV determines the ^{7}Li$(d,p)^8$Li cross section at low energies [20], and is used to normalize the ^{7}Be$(p,\gamma)^8$B cross section. We started from Γ_p and Γ_d values which reproduce the ^{7}Li$(d,p)^8$Li cross section near the resonance, and adjusted Γ_α to account for the structure in the ^{8}Li$(p,\alpha)^5$He cross section at low energies.

For the resonance at 0.62 MeV we used similar Γ_p and Γ_α as in Ref. [11], where this resonance is well observed in the ^{8}Li$(p,\alpha)^5$He reaction. We observe a resonance at $E_{\rm c.m.} = 1.1$ MeV, which was not observed in the (p,α) channel [11], but appears in the (p,d) channels. This resonance is cited in Ref. [21] at the same energy, but decaying only by γ transitions.

The ^{8}Li$(p,\alpha)^5$He cross section presents a broad peak near $E_{\rm c.m.} = 1.7$ MeV, which was already observed in Ref. [11], where two resonances were employed to reproduce the total observed cross section. Ref. [21] also cites two resonances at $E_{\rm c.m.} = 1.69$ and 1.76 MeV. These resonances can also be observed as a minimum in the ^{8}Li$(p,p)^8$Li cross section and as peak in the ^{8}Li$(p,d)^7$Li

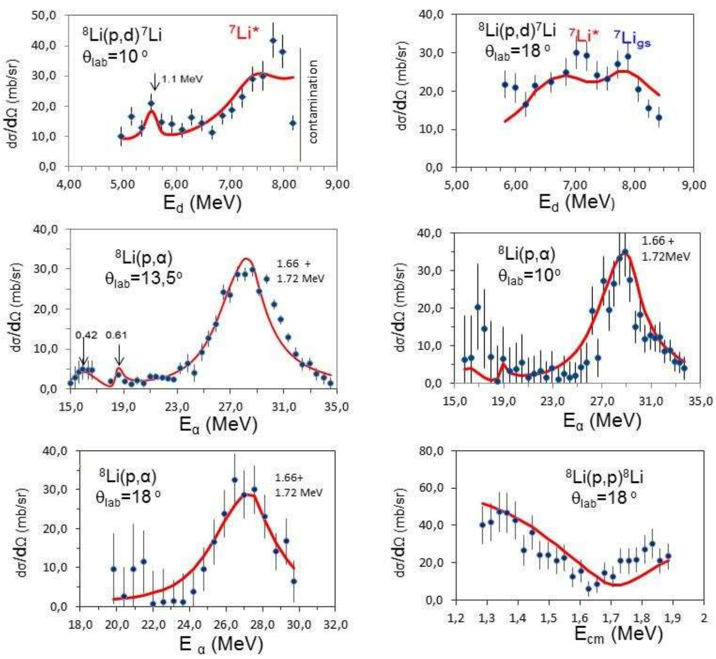

Figure 3: (Color online). This figure presents the experimental cross sections (blue dots), respectively, of the reaction $^8\text{Li}(p,d)^7\text{Li}$ (upper row), of the reaction $^8\text{Li}(p,\alpha)^5\text{He}$ (middle row and lower row) and of the $^8\text{Li}(p,p)^8\text{Li}$ elastic scattering (lower row). Superimposed we include the multi-channel R-matrix calculations (red solid lines), which give the best fit to the data. The detection angles and the energy of the resonances are also indicated on the figures.

cross sections. The contribution of the channel ^{8}Li(p,α)^{5}He* was negligible to the cross sections and we decided to use very small partial widths for all resonances.

The lower lying resonance in our calculations is at $E_{\text{c.m.}} = 1.66 \pm 0.02$ MeV and it has J^π=7/2$^-$ and an orbital angular momentum of $\ell = 2$ for the (p,α), (p,d) and (p,d') channels. It has a large proton width, α and deuteron width, it can practically reproduce by itself the $^8\text{Li}(p,\alpha)^5\text{He}$ cross section, however it is unable to reproduce simultaneously the $^8\text{Li}(p,d)^7\text{Li}$ cross section also. The higher lying resonance in our calculations is at $E_{\text{c.m.}} = 1.72 \pm 0.03$ MeV and it has J^π=5/2$^-$ and an orbital angular momentum of $\ell = 2$ for the (p,α), and (p,d') channels, and ℓ=0 for the (p,d) channel. This resonance is much narrower, but is essential to produce two peaks in the deuteron excitation function. In Figure 4 is shown the fit obtained by using either only the resonance at 1.66 MeV or the resonance at 1.72 MeV. It was impossible to reproduce the data with only one of them, even changing spins, parities and partial widths. In order to improve the absolute value of the $^8\text{Li}(p,p)^8\text{Li}$ reaction we included a background by adding a high lying resonance at $E_{\text{c.m.}} = 5.0$ MeV with J^π=3/2$^+$, Γ_p=8.0 MeV and all other partial widths being zero.

Information on clustering or, in other words, on the deformation of a state, can be inferred from the reduced widths γ^2 in the various channels. When γ^2 exhausts a significant fraction (typically $\approx 10-20\%$) of the Wigner limit ($\gamma_W^2 = 3\hbar^2/2\mu a^2$, where μ is the reduced mass), the reduced width brings out a dominant cluster structure in the corresponding channel. This method has been mostly used in elastic and inelastic scattering to investigate proton-rich nuclei [8, 14]. We calculated the

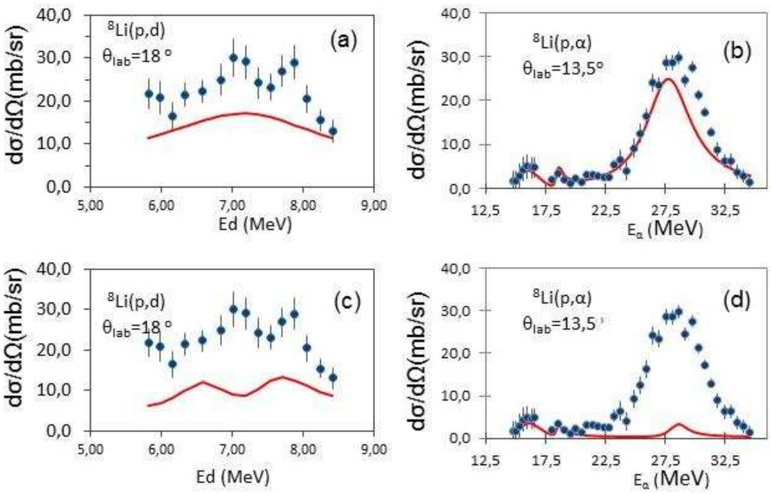

Figure 4: (Color online). This figure presents the experimental cross sections (blue dots), respectively, of the reaction $^8\mathrm{Li}(p,d)^7\mathrm{Li}$ (a,c), and of the reaction $^8\mathrm{Li}(p,\alpha)^5\mathrm{He}$ (b.d). The red solid lines in (a,b) are R-matrix fits with only the resonance of 1.66 MeV, with its parameters given in Table 1. In the figures (c,d) only the resonance at 1.72 MeV was included.

Present							Literature [21]		
E_r	J^π	Γ_p	Γ_α	$\Gamma_{\alpha'}$	Γ_d	$\Gamma_{d'}$	E_r	J^π	Γ
0.42 ± 0.03	$5/2^-$	40 ± 6	25 ± 8	-	150	-	0.40	$(5/2)^-$	200
0.61 ± 0.04	$7/2^+$	1.0	52	-	-	-	0.605	$(7/2)^+$	47
1.10 ± 0.04	$3/2^+$	10	-	-	30	10			
1.66 ± 0.02	$7/2^-$	260	190	-	100	45			
1.72 ± 0.03	$5/2^-$	60	35	-	35	100	1.76	$(5/2)^-$	300 ± 100

Table 1: Resonance properties (energies in MeV, widths in keV). Energies are given with respect to the $^8\mathrm{Li}+p$ threshold.

dimensionless reduced widths $\theta^2= \gamma^2/\gamma_W^2$ for our results and found quite high values: the 1.66 MeV resonance, with J^π=7/2$^-$ has θ_d^2 = 8% and $\theta_{d'}^2 = 7\%$. The 1.72 MeV resonance, has $\theta_{d'}^2 =$ 14%. These large values are typical of cluster states. As ^{7}Li and d are known to present a strong deformation ($\alpha+t$ and $p+n$, respectively), the state observed at $E_{\mathrm{c.m.}} = 1.72$ MeV could be a candidate with a dominant four-body $\alpha+t+p+n$ structure. Moreover it is also the example of a state with excited $^7\mathrm{Li}^*$ core.

5. Conclusions

The high-lying resonances of the ^{9}Be were produced by the ^{8}Li+p reaction, excitation functions of the $^8\mathrm{Li}(p,p)^8\mathrm{Li}$,$^8\mathrm{Li}(p,\alpha)^5\mathrm{He}$ and $^8\mathrm{Li}(p,d)^7\mathrm{Li}$ reactions were measured. Evidence was found for excitation of ^{7}Li in the $^8\mathrm{Li}(p,d)^7\mathrm{Li}$ reaction. We could determine the spin and parity of these resonances, as well as their energies and partial widths with a fair confidence since the existence of six excitation functions for three different reactions constituted a strong constraint on all parameters. The $^{8}\mathrm{Li}(p,d)^{7}\mathrm{Li}$ data suggest a four-body $\alpha+t+p+n$ resonance near $E_x = 18.61$ MeV in ^{9}Be. Its theoretical interpretation is a challenge for cluster models, and it certainly deserves further experimental and theoretical studies. In particular, a similar $^{7}\mathrm{Li}^{*}+d$ resonance with $\ell = 0$ should exist at lower energies.

References

[1] I. Tanihata, H. Savajols, R. Kanungo, *Prog. Part. Nucl. Phys.* **68** (2013) 215 .

[2] S. Gales, *Prog. Part. Nucl. Phys.* **59** (2007) 22.

[3] T. Motobayashi, *Prog. Part. Nucl. Phys.* **59** (2007) 32.

[4] A. Lépine-Szily, R. Lichtenthäler, V. Guimarães, *Eur. Phys. J. A* **50** (2014) 128.

[5] C. Bertulani, A. Gade, *Phys. Rep.* **485** (2010) 195.

[6] I. Tanihata *et al.*, *Phys. Rev. Lett.* **55** (1985) 2676.

[7] O. Sorlin, M. G. Porquet, *Prog. Part. Nucl. Phys.* **61** (2008) 602.

[8] M. G. Pellegriti *et al.*, *Phys. Lett. B* **659** (2008) 864.

[9] A. M. Moro, R. Crespo, *Phys. Rev. C* **85** (2012) 054613.

[10] A. Deltuva, *Phys. Rev. C* **88** (2013) 011601 .

[11] D. R. Mendes Jr. *et al.*, *Phys. Rev. C* **86** (2012) 064321.

[12] A. M. Lane, R. G. Thomas, *Rev. Mod. Phys.* **30** (1958) 257.

[13] P. Descouvemont, D. Baye, *Rep. Prog. Phys.* **73** (2010) 036301.

[14] J. P. Mitchell *et al.*, *Phys. Rev. C* **87** (2013) 054617.

[15] P. Descouvemont, *Eur. Phys. J. A* **12** (2001) 413.

[16] R. Lichtenthäler *et al.*, *Eur. Phys. J. A* **25** (2005) 733.

[17] E. A. Benjamim *et al.*, *Phys. Lett. B* **647** (2007) 30.

[18] D. Mountford *et al.*, *Nucl. Instr. Meth. A* **767** (2014) 359.

[19] C. R. Brune, *Phys. Rev. C* **66** (2002) 044611.

[20] S. Bashkin, *Phys. Rev.* **95** (1954) 1012.

[21] D. R. Tilley *et al.*, *Nucl. Phys. A* **745** (2004) 133.

PoS(INPC2016)223